RESEARCH MEMORANDUM

CONTROL HINGE-MOMENT AND EFFECTIVENESS CHARACTERISTICS OF A HORN-BALANCED, FLAP-TYPE CONTROL ON A 55° SWEPTBACK TRIANGULAR WING OF ASPECT RATIO 3.5 AT MACH NUMBERS OF 1.41, 1.62, AND 1.96

By Lawrence D. Guy

Langley Aeronautical Laboratory
Langley Field, Va.

NATIONAL ADVISORY COMMITTEE
FOR AERONAUTICS

WASHINGTON
January 29, 1953

NATIONAL ADVISORY COMMITTEE FOR AERONAUTICS

RESEARCH MEMORANDUM

CONTROL HINGE-MOMENT AND EFFECTIVENESS CHARACTERISTICS OF A HORN-BALANCED, FLAP-TYPE CONTROL ON A 55° SWEPTBACK TRIANGULAR WING OF ASPECT RATIO 3.5 AT MACH NUMBERS OF 1.41, 1.62, AND 1.96

By Lawrence D. Guy

SUMMARY

An investigation of a horn-balanced, flap-type control mounted on a 55° sweptback, triangular wing of aspect ratio 3.5 was conducted in the Langley 9- by 12-inch supersonic blowdown tunnel. Control hinge moments, and the aerodynamic characteristics of the complete wing-body combination, with and without fences, were obtained over a large range of control deflection and angle of attack at Mach numbers of 1.41, 1.62, and 1.96 and Reynolds numbers of 2.2×10^6, 2.0×10^6, and 1.8×10^6, respectively. Data were also obtained in an experimental nozzle at Mach numbers of 0.72 to 0.82 and Reynolds numbers from 1.9×10^6 to 2.2×10^6, respectively. The effects of control trailing-edge bluntness at supersonic speeds were also examined.

The control exhibited nonlinear variations of hinge moment with both angle of attack and deflection at all Mach numbers. At supersonic speeds the fence greatly reduced the large overbalanced hinge moments due to angle-of-attack loading and greatly reduced the nonlinear variations of hinge moment with deflection. Control trailing-edge bluntness decreased algebraically the control hinge moments at all angles of attack and deflections at supersonic speeds.

The control was effective throughout the range of the investigation which included combined angles of attack and deflection of 40° at a Mach number of 1.96. Neither the increase in trailing-edge thickness nor the addition of a fence was effective at an angle of attack of 0° although both increased the positive rolling effectiveness at larger angles of attack and positive deflections. Both the fence and control trailing-edge bluntness had little effect on the wing minimum drag coefficient at all Mach numbers for which tests were made.

INTRODUCTION

Plain flap-type control surfaces have been used to provide lateral and longitudinal control at transonic and supersonic speeds. The very large hinge moments developed by this type of control surface at high speeds have encouraged research on various means of balancing such controls aerodynamically. Control balance areas extending ahead of the hinge line at the wing tip have been used successfully to reduce control hinge moments at supersonic as well as subsonic speeds. (For example, see refs. 1 and 2.) Such balance arrangements, however, are found to have rather irregular variations of hinge moment with angle of attack and control deflection as well as substantial changes in balance characteristics with Mach number in the transonic and supersonic speed ranges. It is therefore desirable to obtain further information about this type of balance arrangement on high-speed wing-control configurations. In order to furnish such information, an investigation has been made in the Langley 9- by 12-inch supersonic blowdown tunnel on a horn-balanced flap-type control mounted on a 55° sweptback, triangular wing of aspect ratio 3.5 at Mach numbers of 1.41, 1.62, and 1.96 and Reynolds numbers of 2.2×10^{6}, 2.0×10^{6}, and 1.8×10^{6}, respectively. Limited tests were conducted in an experimental nozzle at Mach numbers from 0.72 to 0.82 and Reynolds numbers from 1.9×10^{6} to 2.2×10^{6}, respectively.

The aerodynamic characteristics of the complete semispan model as well as control hinge moments were obtained throughout a maximum control deflection range of 0° to 20° and a maximum angle-of-attack range of $\pm 20^{\circ}$. The effect on control characteristics of blunting the control trailing edge to one-half the hinge-line thickness was examined. Two different size fences, mounted at the parting line between the wing and the tip balance area, were tested in an attempt to improve hinge-moment characteristics.

SYMBOLS

C_L lift coefficient, $\frac{\text{Lift}}{qS}$

C_D drag coefficient, $\frac{\text{Drag}}{qS}$

C_m pitching-moment coefficient, $\frac{\text{Pitching moment}}{qS\bar{c}}$, (pitching-moment reference axis located at $0.25\bar{c}$)

$C_{l_{gross}}$ gross rolling-moment coefficient, $\frac{\text{Semispan-model rolling moment}}{2qSb}$, (reference axis shown in fig. 1)

C_h control hinge-moment coefficient, $\frac{\text{Hinge moment}}{qb_f\bar{c}_f^{\,2}}$

C_l, ΔC_L, ΔC_m increment in gross rolling-moment coefficient, lift coefficient, and pitching-moment coefficient due to deflection of control surface

q free-stream dynamic pressure

S semispan wing area (including area blanketed by test body)

c local wing chord

$\bar{c}$ mean aerodynamic chord of wing

$\bar{c}_f$ mean aerodynamic chord of portion of control behind hinge line

b wing span, twice distance from rolling-moment reference axis to wing tip

b_f control-surface span, 60 percent $b/2$

α angle of attack measured with respect to free stream

δ control-surface deflection measured perpendicular to hinge line from wing chord plane at control inboard end

R Reynolds number based on mean aerodynamic chord of wing

M Mach number

Subscripts:

α slope of curve of coefficient plotted against α; $dC_h/d\alpha$, $dC_L/d\alpha$, and so forth

δ slope of curve of coefficient plotted against δ; $dC_l/d\delta$, $dC_h/d\delta$, and so forth

DESCRIPTION OF MODEL

The principal dimensions of the semispan-wing—body combination are given in figure 1 and a photograph of the model is shown in figure 2. The semispan wing was of triangular plan form having 55° leading-edge sweepback and an aspect ratio of 3.5. A horn-balanced, flap-type control was hinged at the 70.0-percent-chord line and spanned the outboard 60 percent of the wing semispan. The inboard half of the control span comprised 31.7 percent of the local wing chord and the outboard half comprised 100 percent of the wing chord.

The main wing panel was made of heat-treated steel. The wing ahead of the control surface had NACA 65A005 airfoil sections parallel to the free-stream direction. Inboard of the control surface the wing thickness was increased to the rear of the 20-percent-chord station to permit installation of an internal strain-gage beam. Ordinates are given in table I.

Two control surfaces of identical plan form and machined from heat-treated steel were used in the investigation. The basic control surface had NACA 65A005 airfoil sections in planes parallel to the free-stream direction. A second control had NACA 65A005 airfoil sections forward of the hinge line but was slab-sided behind the hinge line with a trailing-edge thickness of one-half the hinge-line thickness.

The investigation included tests of two fences. One, a full-chord fence having a constant height of 24.2 percent chord above the control-chord plane, was mounted on the control surface at the outboard wing-control parting line. The other fence, extending 24.2 percent chord above the wing-chord plane at the leading edge and tapering to zero height at the hinge line, was mounted on the wing at the outboard wing-control parting line.

A test body consisting of a half body of revolution together with a 0.25-inch Micarta shim was integral with the main wing panel for all tests.

TUNNEL

The tests were conducted in the Langley 9- by 12-inch supersonic blowdown tunnel which operates from the compressed air of the Langley 19-foot pressure tunnel. The absolute stagnation pressure of the air entering the test section ranges from 2 to $2\frac{1}{3}$ atmospheres. The compressed air is conditioned to insure condensation-free flow in the test section by being passed through a silica-gel drier and then through banks of finned electrical heaters. Criteria for condensation-free flow were obtained from reference 3. Turbulence damping screens are located in the settling chamber. Three test-section Mach numbers are provided by interchangeable nozzle blocks.

Deviations of flow conditions in the test section with tunnel clear, determined from extensive calibration tests and reported in reference 4, are presented in the following table along with properties of the conditioned air:

Variable	Nominal Mach number		
	1.41	1.62	1.96
Maximum deviation in Mach number	±0.02	±0.01	±0.02
Maximum deviation in ratio of static to stagnation pressure, percent	±2.0	±1.3	±2.2
Maximum deviation in ratio of dynamic to total pressure, percent	±0.4	±0.2	±0.3
Maximum deviation in stream angle, deg . .	±.25	±.20	±.20
Maximum dewpoint temperature, °F	20	-5	-20
Minimum stagnation temperature, °F	120	135	165

Limited tests were made in an experimental nozzle operating at subsonic Mach numbers from 0.72 to 0.82. Details of the flow characteristics of this nozzle were unknown, but wall-pressure measurements indicated the tunnel-clear test-section Mach number variation was about ±0.01. The subsonic test-section Mach number indicated by wall pressures decreased about 0.02 as the angle of attack was increased from 0° to 15°. The flow conditions were believed to be sufficiently uniform to permit evaluation of changes in wing and control characteristics caused by addition of a fence to the wing.

TEST TECHNIQUE

The model was cantilevered from a five-component strain-gage balance set flush with the tunnel floor. The model and the balance rotated together as the angle of attack was changed. The aerodynamic forces and moments on the semispan-wing—body combination were measured with respect to the body axes and then rotated to the wind axes. The body consisted of a half body of revolution mounted on a 0.25-inch shim; the shim was used to minimize the tunnel-wall boundary-layer effects on the flow over the surface of the body of revolution (ref. 5). A clearance gap of 0.010 to 0.020 inch was maintained between the fuselage shim and the tunnel floor.

The hinge moments of the horn-balanced control surface were measured by means of an electrical strain-gage beam buried in the main wing panel adjacent to the inboard end of the control surface. The control was hinged to the main wing panel by a 0.030-inch-diameter steel pin just inboard of the control balance area and by a 0.060-inch-diameter steel pin at its inboard end. The control deflection was fixed by means of a positioning pin soldered to the control surface and fitted into a hole in the strain-gage beam. The control deflection was changed for each series of tests by changing the positioning pin.

ACCURACY OF DATA

An estimate of the probable errors introduced in the present data by instrument-reading errors, measuring-equipment errors, and calibration errors are presented in the following table:

Variable—	Moderate load conditions	Maximum load conditions
α, deg . . .	±0.04	±0.06
δ, deg . . .	±0.1	±0.2
C_L	±0.005	±0.010
C_l	±0.0005	±0.0015
C_m	±0.001	±0.003
C_D	±0.001	±0.004
C_h	±0.005	±0.008

Because of the thinness of the control airfoil sections and the consequent control flexibility, the determination of the mean angular control deflection due to load has not been attempted since an analysis of the aeroelastic characteristics of the control would be required. The control deflections, against which the data of the present report are plotted, were measured at a point on the control trailing edge adjacent to the main wing panel.

The absolute values of the wing-body force and moment coefficients include loads on the arbitrary test body and are not applicable to configurations having more conventional body shapes. The variation of the wing-body characteristics with control deflection, however, should apply to more conventional configurations. It is believed that the increased thickness of the wing inboard of the control had negligible effect on control characteristics.

RESULTS AND DISCUSSION

Representative basic aerodynamic coefficients of the semispan model plotted against control deflection for various angles of attack at Mach numbers of 1.41, 1.62, and 1.96 are presented in figure 3. Comparative data obtained at Mach numbers of 0.72, 1.41, and 1.96 for the model with and without fences are presented in the form of cross plots in figures 4 and 5. In figure 6 data obtained for the model with a control having thickened trailing edges are compared with those of the basic wing-control configuration at $M = 1.41$ and $M = 1.96$. In these later figures the signs of the test values of angle of attack, control deflection, and model force and moment coefficients obtained at negative angles of attack and positive control deflections have been arbitrarily reversed for convenience of presentation. This was permissible by reason of model symmetry.

Control Characteristics of Basic Configuration

Hinge moment.- Cross plots of fence-off control hinge-moment coefficient against angle of attack for zero control deflection (fig. 4) show large nonlinear variations and indicate that the control was overbalanced (the center of pressure was ahead of the hinge line) over most of the angle-of-attack range at all Mach numbers of the investigation. The amounts of overbalance, shown by the magnitude of the hinge-moment coefficients, were much greater at $M = 0.72$ than at the supersonic Mach numbers, indicating the typical rearward shift of the center of pressure with increasing Mach number. At $M = 0.72$ the major effect of the fences was to extend the linear portion of the curve which passes through zero and to delay the break to a slightly higher angle of attack. At supersonic Mach numbers, sizable reductions in the values of hinge-moment coefficients for low to moderate angles of attack were caused by the addition of either fence. The partial-chord fence, which extended only from the wing leading edge to the hinge line, however, was more effective than the larger fence in reducing the amount of overbalance at supersonic speeds. In fact, at $M = 1.96$ with the small fence on, zero hinge moments were obtained between $\pm 10^{\circ}$ angle of attack for the undeflected control. The effects of the fences, indicated in figure 4, are in agreement with those of reference 2 which showed that a full-chord fence, similar to the one of the present report, mounted at the parting line of a half-delta tip control on a 60° delta wing caused changes in $C_{h_{\alpha}}$ consistent with a rearward movement of the control center of pressure at Mach numbers from 1.41 to 1.96.

Figure 5(a) presents the hinge-moment variation with deflection of the control with and without the partial-chord fence for several angles of attack at Mach numbers of 0.72, 1.41, and 1.96. The fence-off data show that for positive control deflections the control hinge moment due only to control deflection was overbalanced (positive values of C_{h_δ}) at $M = 0.72$ but was underbalanced (negative values of C_{h_δ}) at Mach numbers of 1.41 and 1.96. The negative values of C_{h_δ} at supersonic speeds were essentially constant with control deflection except for negative deflections at angles of attack above zero. As shown for angles of attack of 8° and 16°, the values of C_{h_δ} increased with increasing negative control deflection and became positive at some deflection. The magnitude of this deflection increased with increasing angle of attack and decreasing Mach number. Reference 2 showed that this increase in values of C_{h_δ} at negative control deflection appeared to be typical of control arrangements having tip balance areas extending to the wing leading edge.

At the supersonic Mach numbers the addition of the small fence in general reduced the nonlinear variations of hinge moment with control deflection. For negative control deflections, positive values of C_{h_δ} were delayed by the fence to angles of attack greater than 16° (available only at $M = 1.96$) and control deflections greater than -16° (the maximum of the tests). For positive control deflections the fence had small, although somewhat erratic, effects on the parameter C_{h_δ}. At $M = 0.72$ addition of the fence increased C_{h_δ} slightly at $\alpha = 0^{\circ}$. At angles of attack greater than 0°, as shown for $\alpha = 8^{\circ}$, the break in the curve where values of C_{h_δ} became negative occurred at a lower control deflection with the fence on than with the fence off.

Effectiveness.- The control, with fence off, was effective in producing an increase in rolling moment with an increase in control deflection throughout the angle-of-attack and control-deflection ranges as shown in figure 5(b) and in more detail in figure 3(b). The variation of rolling moment with control deflection at zero angle of attack was nearly linear throughout the deflection range of the tests. For positive control deflections, increasing the angle of attack or control deflection from zero tended to decrease the parameter C_{l_δ} although the decrease with increasing deflection was small at supersonic speeds. For angles of attack and control deflections of opposite sign the variation of C_{l_δ} with either α or δ was small for angles of attack numerically less than 12° (see fig. 3(b)). At larger angle of attack C_{l_δ} again decreased as the angle of attack increased in magnitude.

The addition of the fence had small effects on rolling-moment variation with deflection at zero angle of attack. At larger angles of attack and positive control deflections the rolling effectiveness parameter C_{l_δ} was increased by the addition of the fence throughout the Mach number range of the investigation. At negative control deflections C_{l_δ} was unaffected by the fence except at $M = 1.96$ where the fence caused a decrease in values of C_{l_δ} that was nearly constant with angle of attack for angles of attack of 8° and higher.

The effects of the fence on the increment of lift due to control deflection (fig. 5(c)) were small and within the accuracy of the data, except at $\alpha = 8^{\circ}$ at $M = 0.72$ where an increase in ΔC_L similar to the increase in C_l occurred.

The data in figure 5(d) show that the addition of the fence had negligible effect on the increment in pitching moment due to control deflection at zero angle of attack. At larger angles of attack the fence caused changes in the variation of ΔC_m with δ consistent with a rearward shift in center of pressure at all control deflections throughout the Mach number range of the investigation.

Effects of Control Trailing-Edge Bluntness on Control Characteristics

Figure 6 presents the variation with deflection of hinge-moment, rolling-moment, lift, and pitching-moment characteristics at $M = 1.41$ and $M = 1.96$ for two controls differing only in trailing-edge thickness. Increasing the control trailing-edge thickness to one-half the hinge-line thickness decreased algebraically the control hinge moments at all angles of attack and positive control deflections. For most negative control deflections, however, trailing-edge bluntness had little effect on the hinge moments. Trailing-edge bluntness also caused small algebraic decreases in values of C_{h_α} at small control deflections as shown by the decrement in hinge moment due to bluntness. These results are in agreement with those of the investigation of reference 6 which showed that increasing the thickness of an unbalanced aileron on a sweptback wing to one-half the hinge-line thickness caused larger negative values of both C_{h_α} and C_{h_δ} for small angles of attack and moderate control deflections at $M = 1.90$.

The data of the present report show that increasing the trailing-edge thickness had negligible effect on rolling moment at $\alpha = 0^{\circ}$ at Mach numbers from 1.41 to 1.96 although reference 6 showed increased aileron rolling effectiveness at $M = 1.90$. At larger angles of attack, however, the blunted control of the present report, in general, produced higher values of rolling-moment coefficient than the basic control. It may be that the increment in rolling moment due to increased trailing-edge thickness is not entirely attributable to the aerodynamic effects of bluntness but may in part be due to increased stiffness of the control since the increment increased with increasing angle of attack plus deflection and also with increasing dynamic pressure (decreasing Mach number for the range between $M = 1.41$ and $M = 1.96$). For negative control deflections at angles of attack above 8° ($M = 1.96$ only), the values of C_{l_δ} are numerically smaller for the blunt control than for the basic control. The reason for this is not clearly understood although this decrease in rolling moment with the increase in trailing-edge thickness is accompanied by a decrease in ΔC_L (fig. 6(b)).

With the exception just noted, figure 6(b) shows only minor effects of trailing-edge bluntness on the variations of ΔC_L and ΔC_m with control deflection.

The effects of the small fence and of control trailing-edge bluntness on the variation with Mach number of the control characteristics at zero angle of attack and deflection are summarized in figure 7.

Wing Characteristics

Figure 8 presents the variation with Mach number of the lift, drag, and pitching-moment characteristics at $\delta = 0^{\circ}$ and of $(L/D)_{max}$ of the model with and without the small fence and also of the model with the basic control replaced by the blunt trailing-edge control. No data were obtained at subsonic speeds for the blunt control. Although the absolute values of the wing-body parameter include effects of the somewhat arbitrary test body, the results of adding a fence or thickening the control trailing edge should be applicable to configurations having more conventional body shapes.

Neither the addition of the fence nor control trailing-edge bluntness had any large effects on the wing-body characteristics at the Mach numbers of the tests. Small increases in the values of the minimum drag coefficient (about 0.001 at all Mach numbers) were caused by both the addition of the fence and the increased trailing-edge thickness of the blunt control. These drag increases were of the same order as the experimental accuracy of the tests. The slight decreases in $(L/D)_{max}$ were attributable to these small drag increases since C_{L_α} at $\alpha = 0^{\circ}$ was unaffected by the fence or by control trailing-edge bluntness and the curves were linear to the point of $(L/D)_{max}$. The fence caused a small rearward shift in center of pressure at the subsonic speeds as shown by the more negative values of dC_m/dC_L but had negligible effect at supersonic Mach numbers. Values of dC_m/dC_L for the model with the blunt trailing-edge control were slightly larger than for the model with the basic control.

CONCLUDING REMARKS

An investigation of a horn-balanced, flap-type control, with and without fences, mounted on a 55° sweptback, triangular wing of aspect ratio 3.5 was made at Mach numbers of 1.41, 1.62, and 1.96. Comparative data for the model with and without fences were obtained in an experimental nozzle at Mach numbers from 0.72 to 0.82. The effects of control trailing-edge thickness were examined at the supersonic Mach numbers. The following results were indicated.

The control exhibited nonlinear variations of hinge moment with both angle of attack and deflection throughout the range of the investigation. At supersonic speeds the fence greatly reduced the large overbalanced hinge moments due to angle-of-attack loading and greatly reduced the nonlinear variations of hinge moment with deflection. Control trailing-edge bluntness decreased algebraically the control hinge moments at all angles of attack and deflection at supersonic speeds.

The control was effective throughout the range of the investigation which included combined angles of attack and deflection of 40° at a Mach number of 1.96. Although neither the increase in trailing-edge thickness nor the addition of the fence was effective at an angle of attack of 0°, both increased the rolling effectiveness C_{l_δ} at larger angles of attack and positive deflections. A decrease in C_{l_δ}, however, was evident at the highest Mach number at negative deflections. Both the fence and control trailing-edge bluntness had little effect on the wing minimum drag coefficient at all Mach numbers for which tests were made.

Langley Aeronautical Laboratory,
National Advisory Committee for Aeronautics,
Langley Field, Va.

REFERENCES

1. Stone, David G.: Comparisons of the Effectiveness and Hinge Moments of All-Movable Delta and Flap-Type Controls on Various Wings. NACA RM L51C22, 1951.

2. Guy, Lawrence D.: Control Hinge-Moment and Effectiveness Characteristics of a 60° Half-Delta Tip Control on a 60° Delta Wing at Mach Numbers of 1.41 and 1.96. NACA RM L52H13, 1952.

3. Burgess, Warren C., Jr., and Seashore, Ferris L.: Criterions for Condensation-Free Flow in Supersonic Tunnels. NACA TN 2518, 1951.

4. May, Ellery B., Jr.: Investigation of the Effects of Leading-Edge Chord-Extensions on the Aerodynamic and Control Characteristics of Two Sweptback Wings at Mach Numbers of 1.41, 1.62, and 1.96. NACA RM L50L06a, 1951.

5. Conner, D. William: Aerodynamic Characteristics of Two All-Movable Wings Tested in the Presence of a Fuselage at a Mach Number of 1.9. NACA RM L8H04, 1948.

6. Sivells, James C., and Goin, Kennith L.: Experimental and Calculated Hinge Moments of Two Ailerons on a 42.7° Sweptback Wing at a Mach Number of 1.9. NACA RM L8K24a, 1949.

TABLE I.- ORDINATES FOR AIRFOIL SECTION INBOARD OF THE

40-PERCENT WING-SEMISPAN STATION

[Stations and ordinates given in percent airfoil chord in free-stream direction; section symmetrical about chord line.]

Station	Ordinate
0	0
1.25	.598
2.50	.818
5.0	1.094
7.5	1.326
10	1.520
15	1.828
20	2.062
45	3.130
50	3.295
55	3.395
60	3.439
65	3.420
70	3.340
75	3.180
80	2.905
100	1.720

NACA

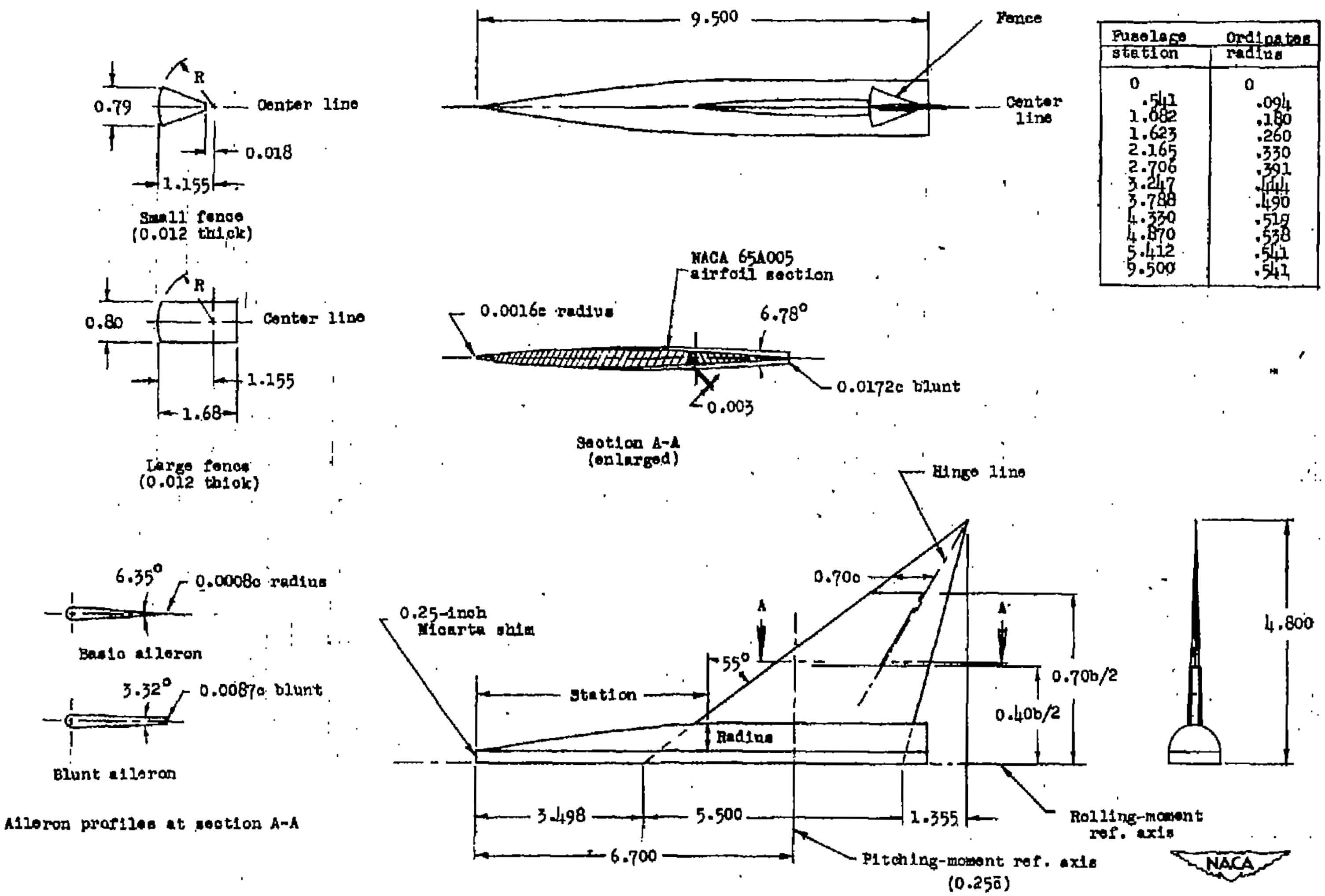

Fuselage station	Ordinates radius
0	0
.541	.094
1.082	.180
1.623	.260
2.165	.330
2.706	.391
3.247	.444
3.788	.490
4.330	.519
4.870	.538
5.412	.541
9.500	.541

Figure 1.- Details of semispan-wing—body combination. Aspect ratio, 3.5; mean aerodynamic chord, 3.667 inches; semispan, 4.800 inches, half wing area, 13.20 square inches. (All dimensions in inches.)

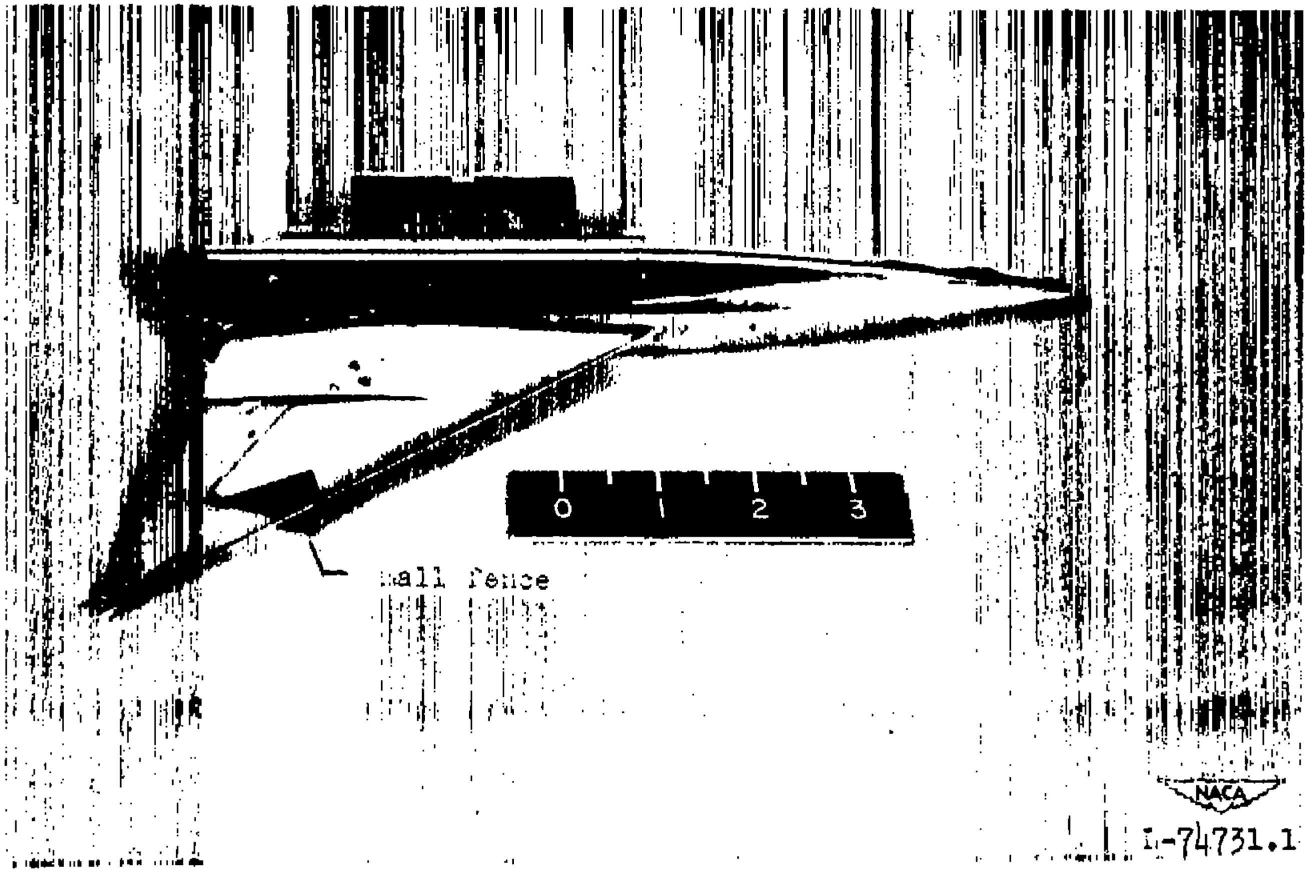

Figure 2.- Photograph of test model.

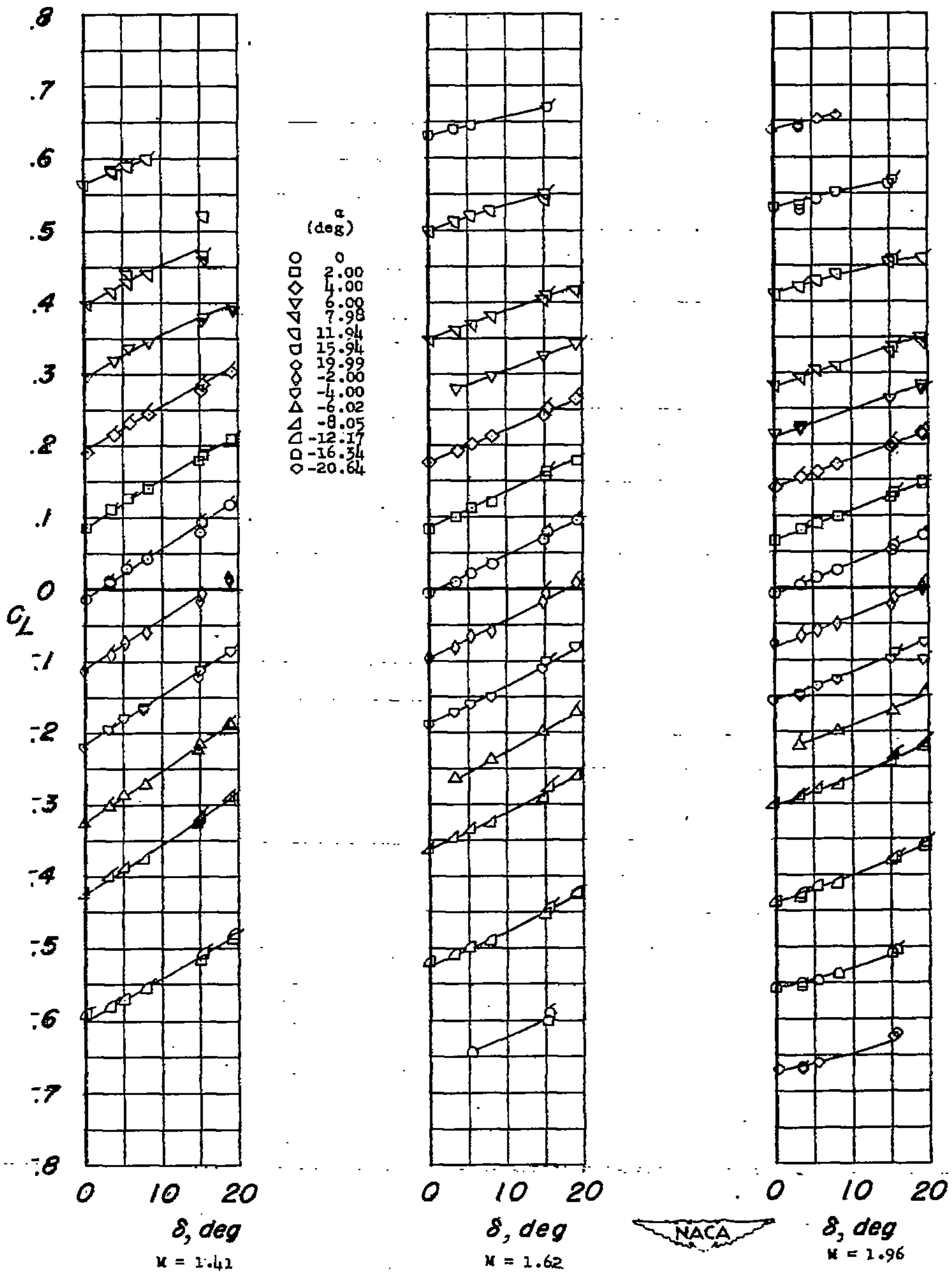

(a) C_L plotted against δ.

Figure 3.- Aerodynamic characteristics of a semispan-wing—body combination with tip horn-balanced trailing-edge control surface. $R = 2.2 \times 10^6$, $R = 2.0 \times 10^6$, and $R = 1.8 \times 10^6$; M = 1.41, M = 1.62, and M = 1.96, respectively. Basic aileron; fence off. Flagged symbols denote repeat tests.

[redacted]

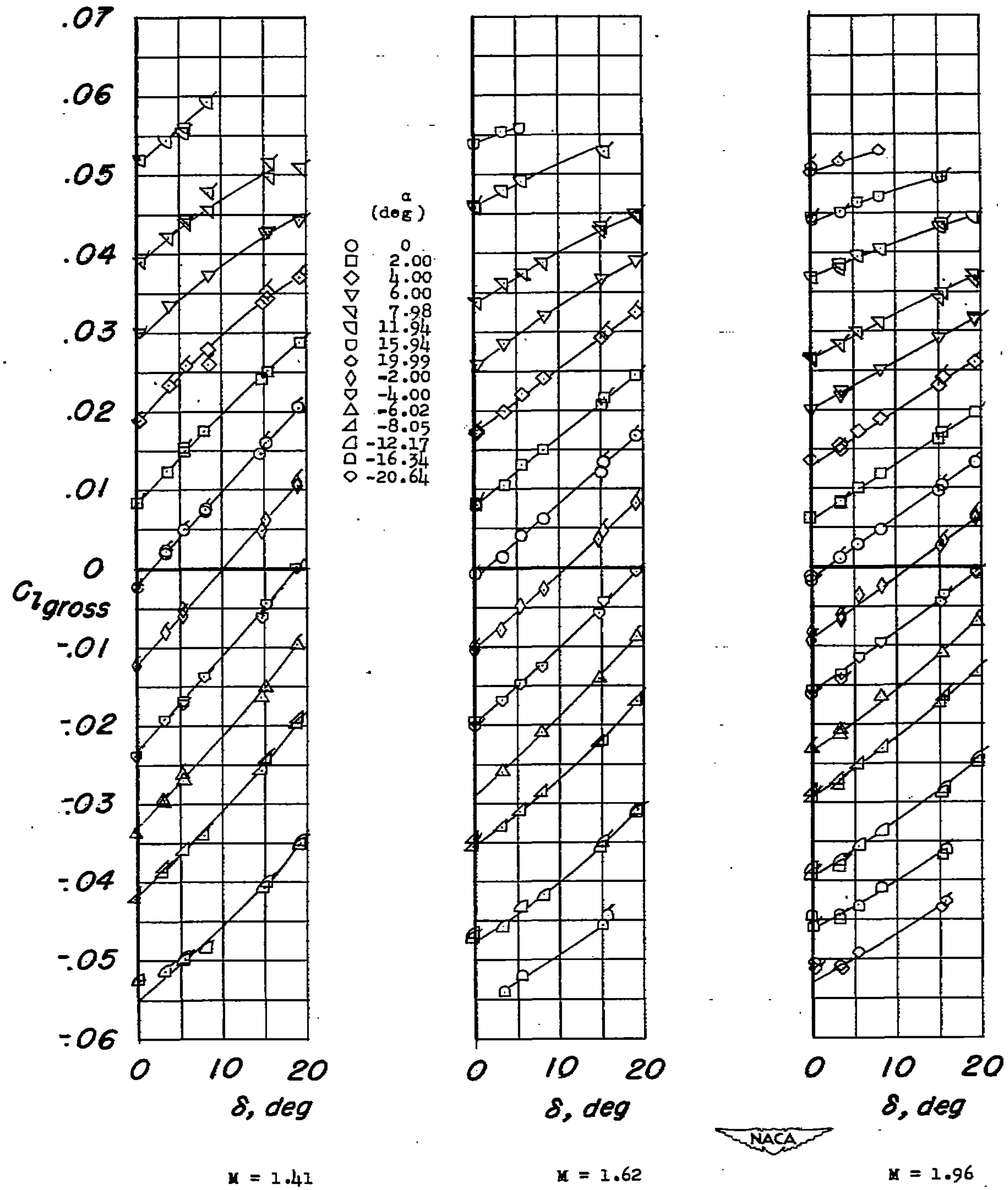

(b) $C_{l_{gross}}$ plotted against δ.

Figure 3.- Continued.

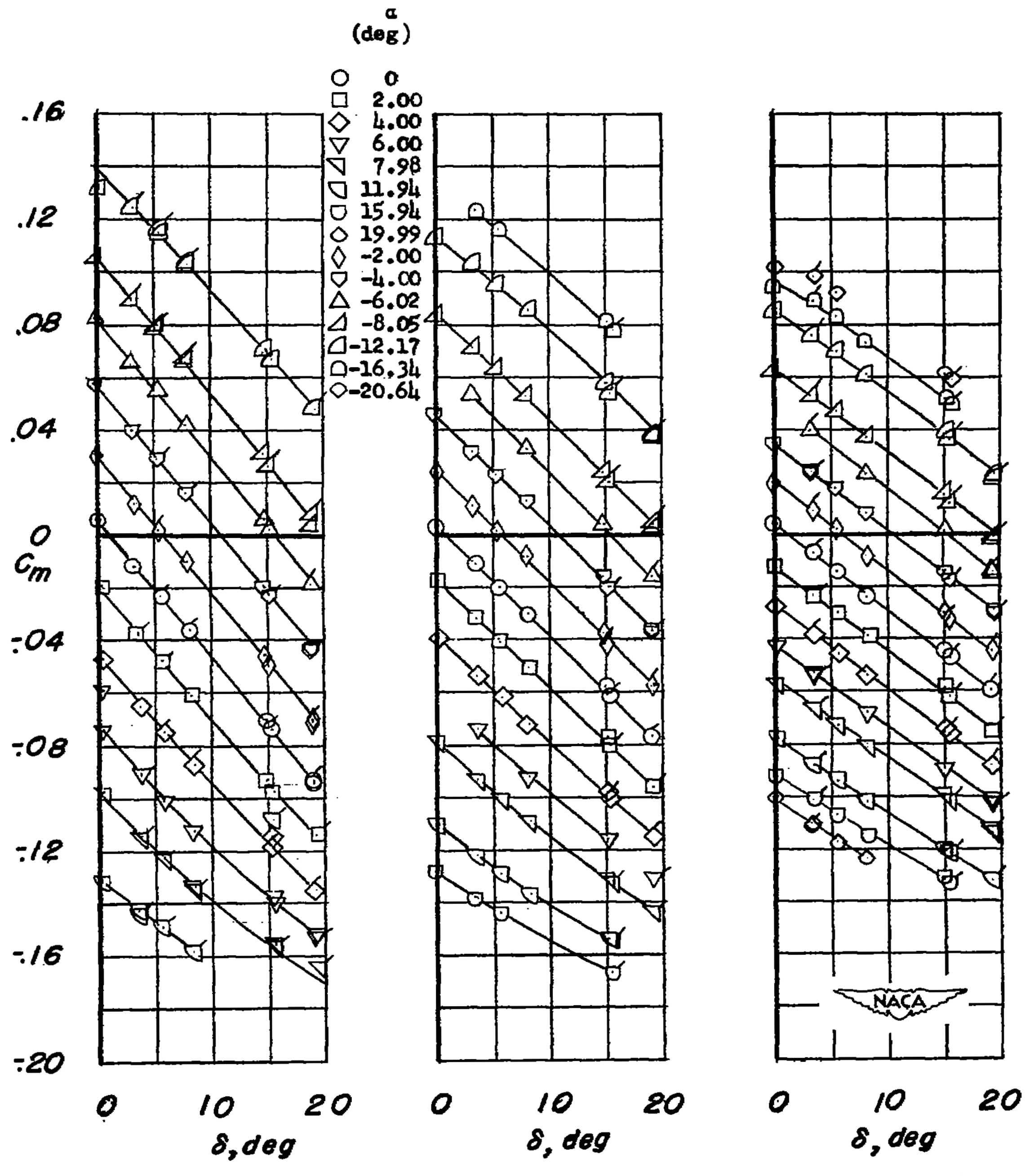

(c) C_m plotted against δ.

Figure 3.- Continued.

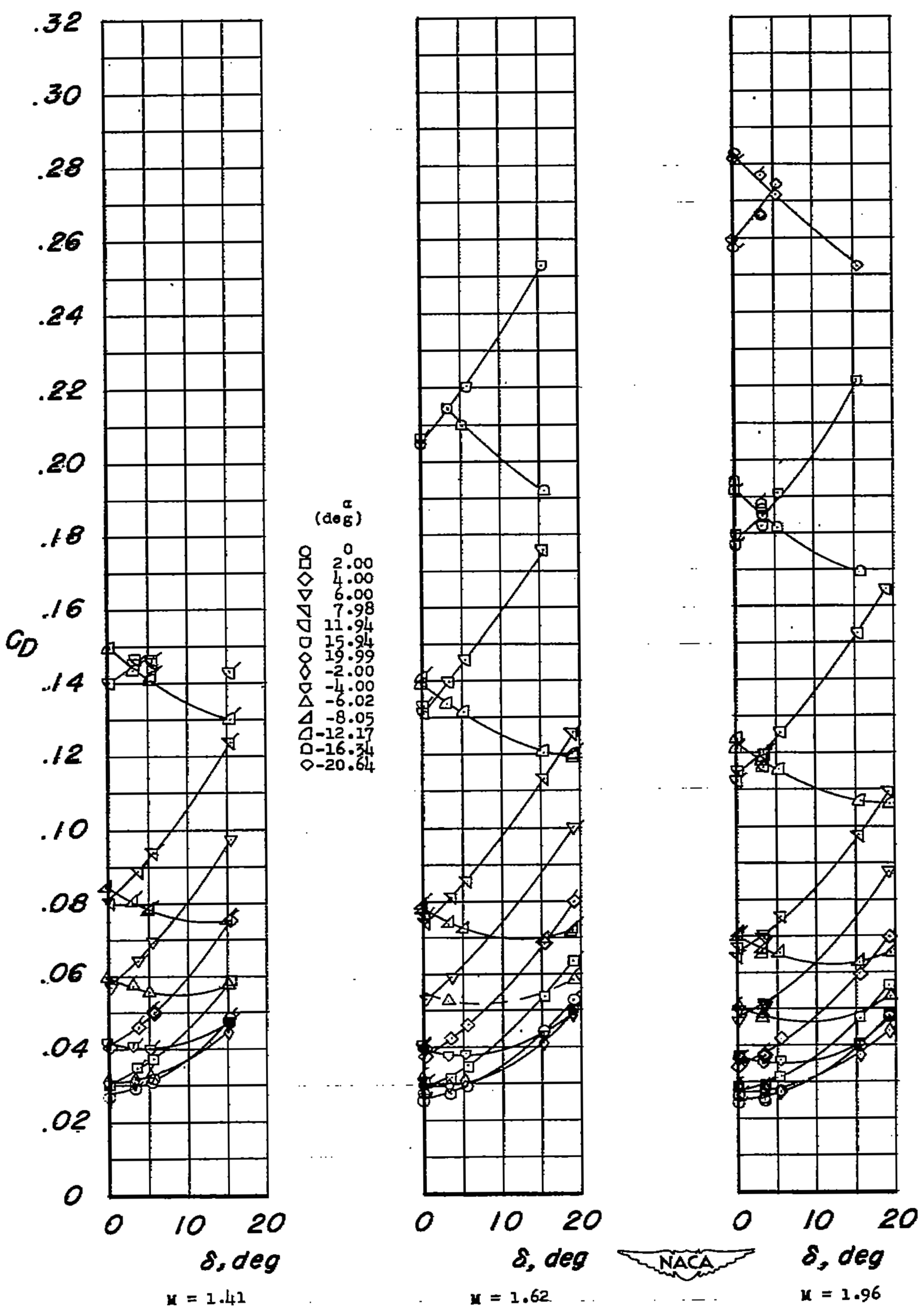

(d) C_D plotted against δ.

Figure 3.- Continued.

[redacted]

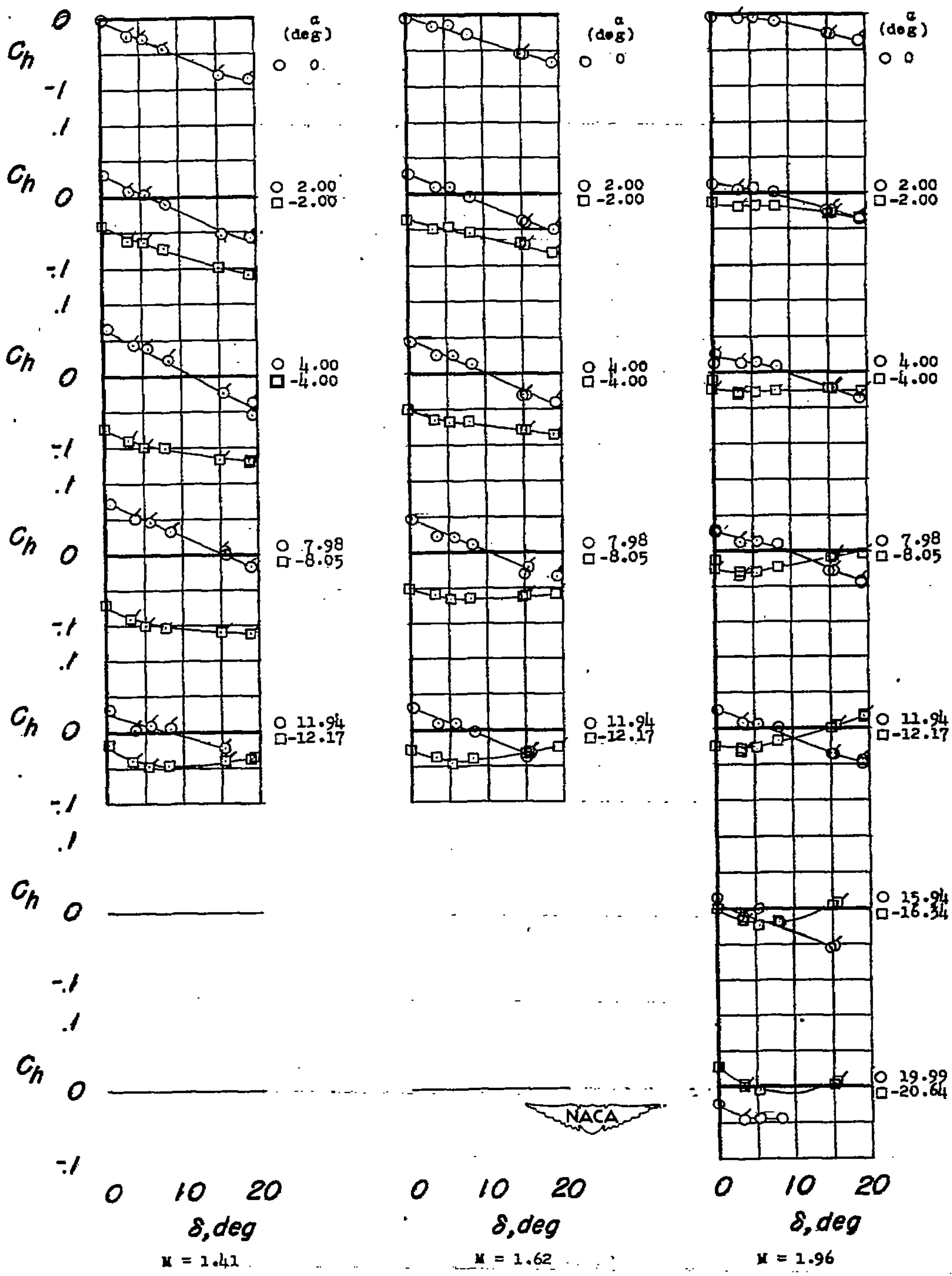

(e) C_h plotted against δ.

Figure 3.- Concluded.

[redacted]

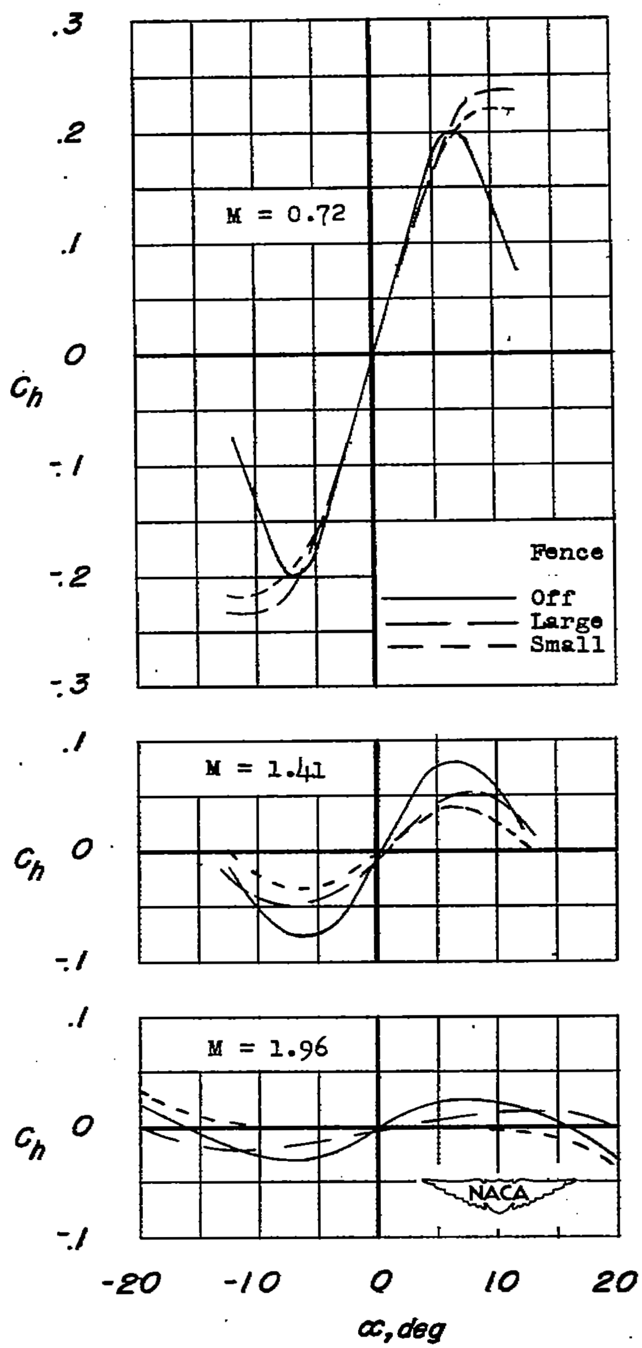

Figure 4.- Effects of a full-chord fence and a partial-chord fence on the control hinge-moment variation with angle of attack. $\delta = 0$; $R = 1.9 \times 10^6$, $R = 2.2 \times 10^6$, and $R = 1.8 \times 10^6$; $M = 0.72$, $M = 1.41$, and $M = 1.96$, respectively. Basic aileron.

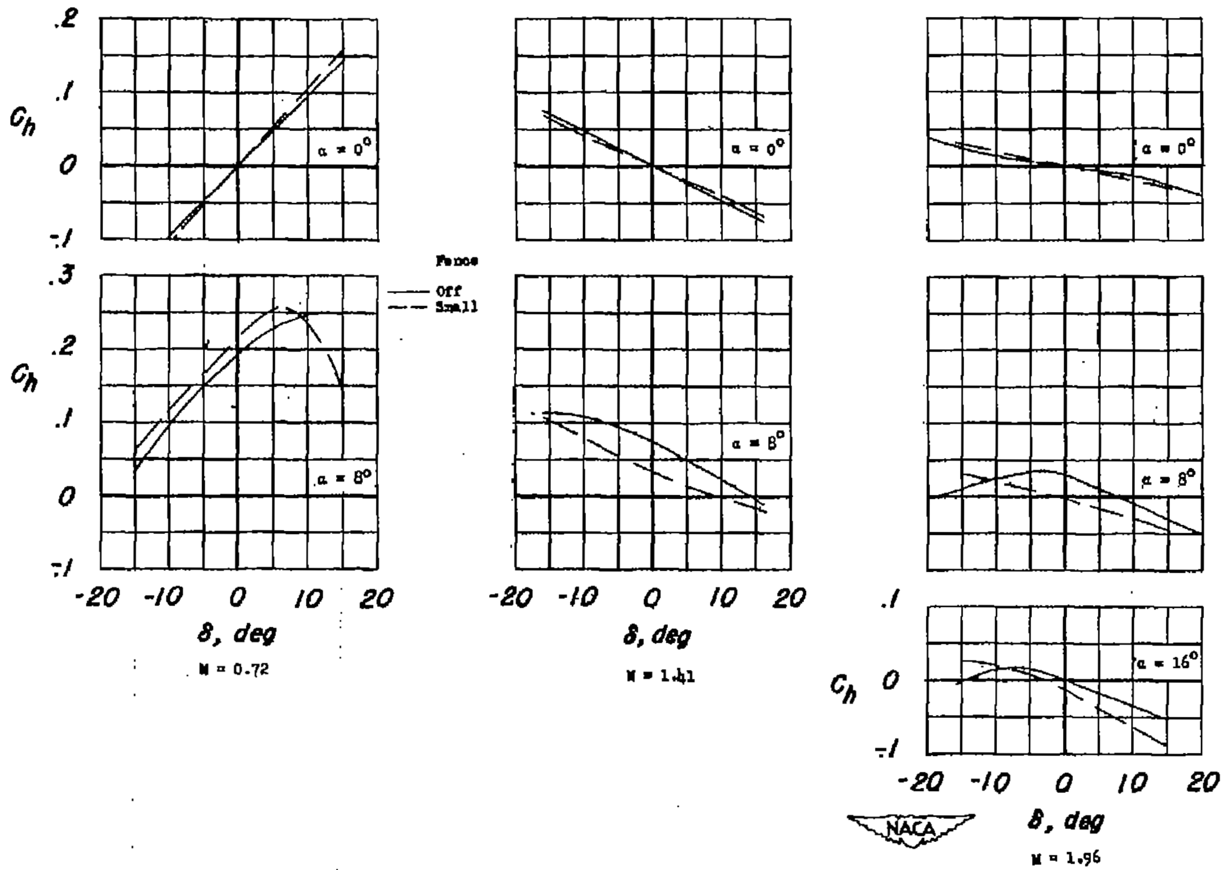

(a) C_h plotted against δ.

Figure 5.- Effects of a fence on the variation with control deflection of hinge moment, rolling moment, and increments of lift and pitching moment due to deflection. Basic control. $R = 1.9 \times 10^6$, $R = 2.2 \times 10^6$, and $R = 1.8 \times 10^6$; M = 0.72, M = 1.41, and M = 1.96, respectively.

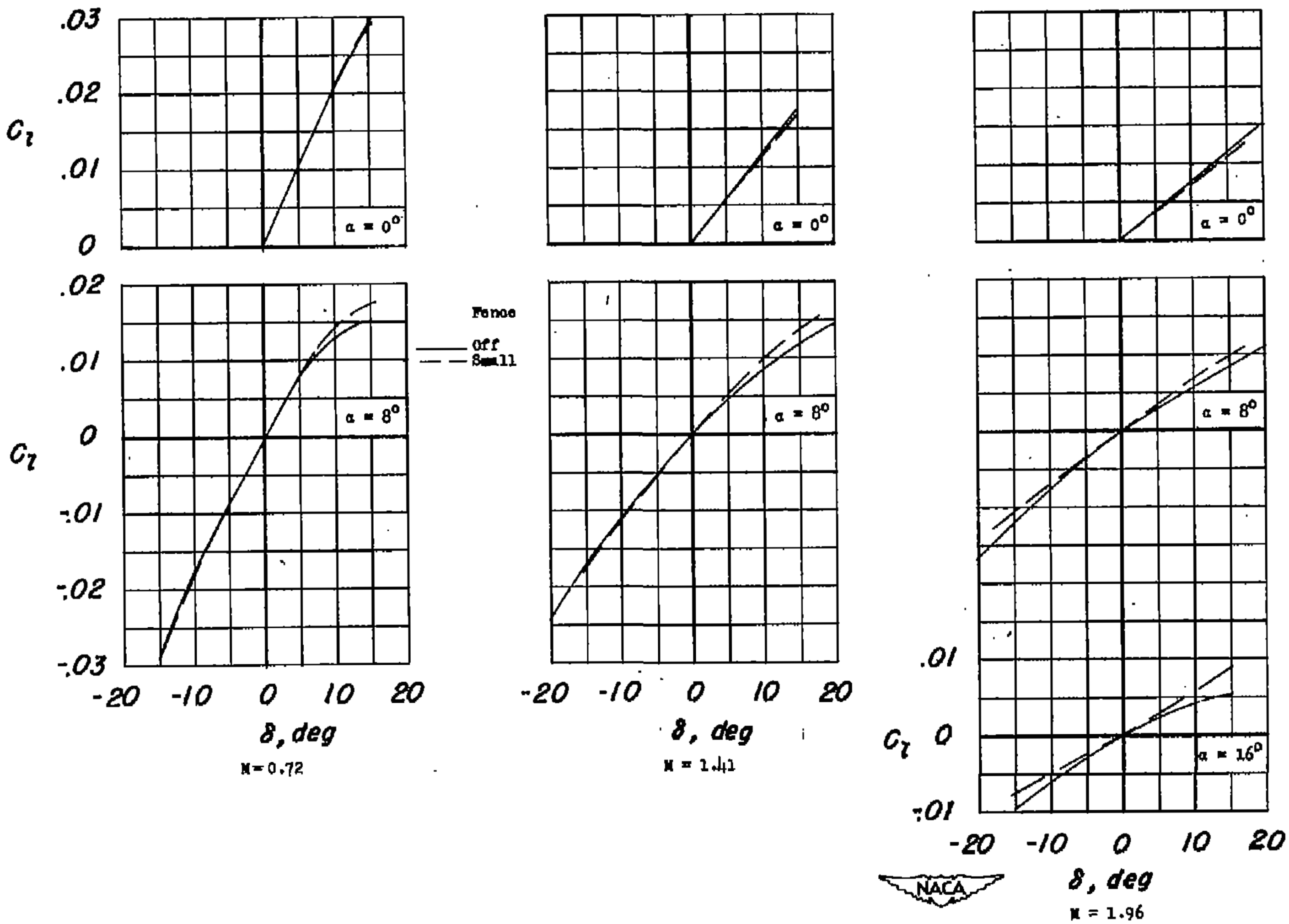

(b) C_l plotted against δ.

Figure 5.- Continued.

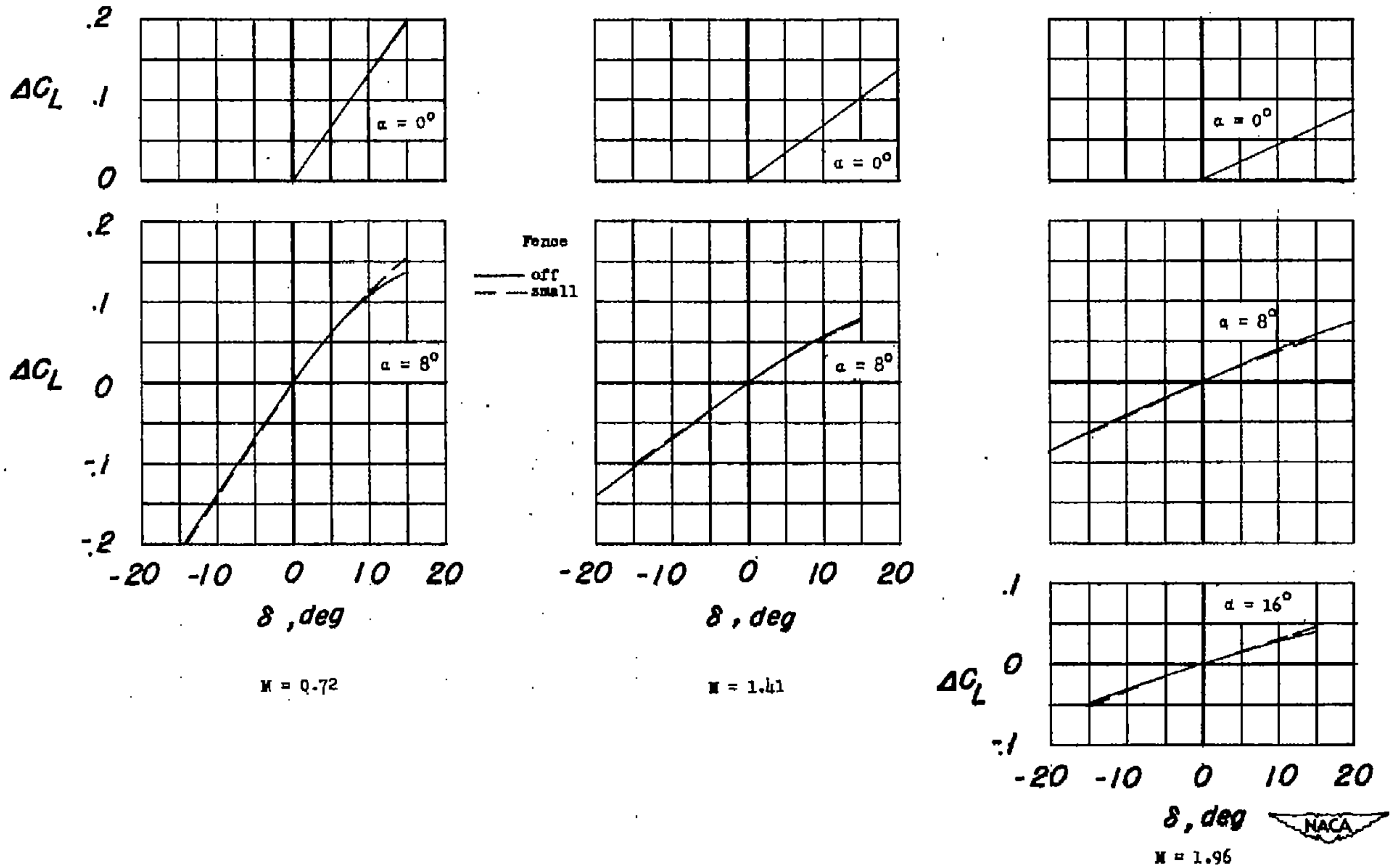

(c) ΔC_L plotted against δ.

Figure 5.- Continued.

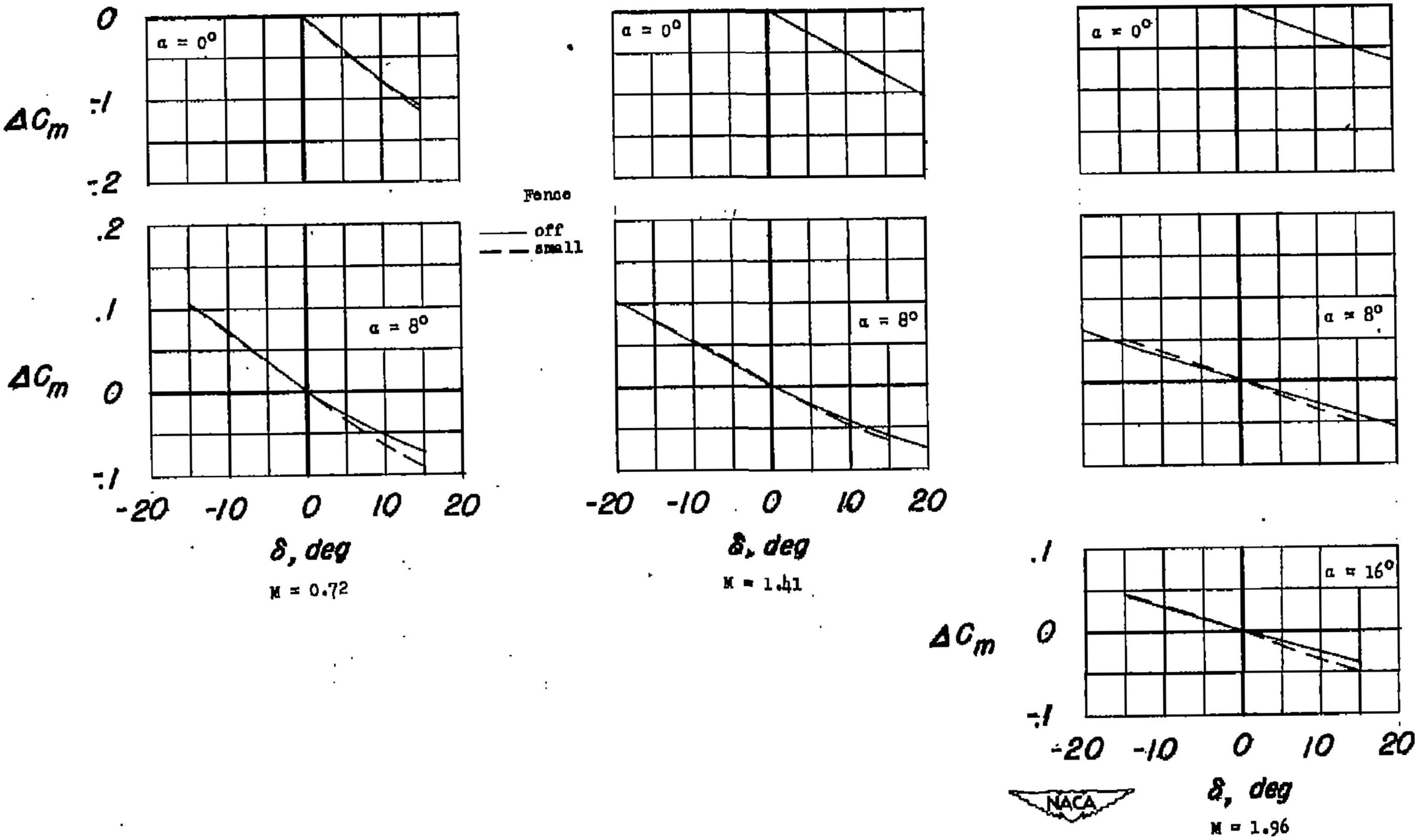

(d) ΔC_m plotted against δ.

Figure 5.- Concluded.

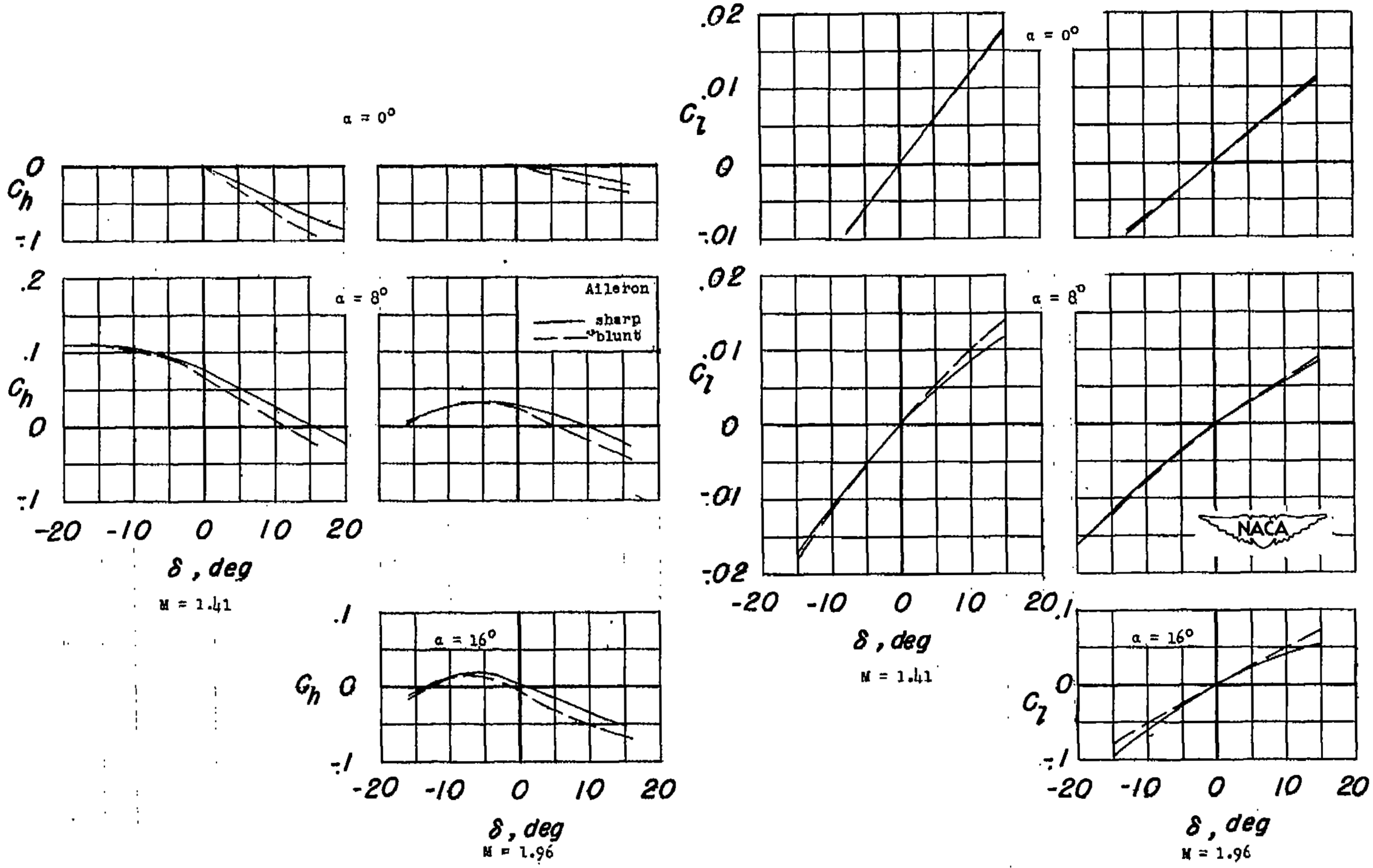

(a) C_h and C_l plotted against δ.

Figure 6.- The variation with control deflection of hinge moment, rolling moment, and increments of lift and pitching moment due to deflection for two controls. $R = 2.2 \times 10^6$ and $R = 1.8 \times 10^6$; $M = 1.41$ and $M = 1.96$, respectively. Fence off.

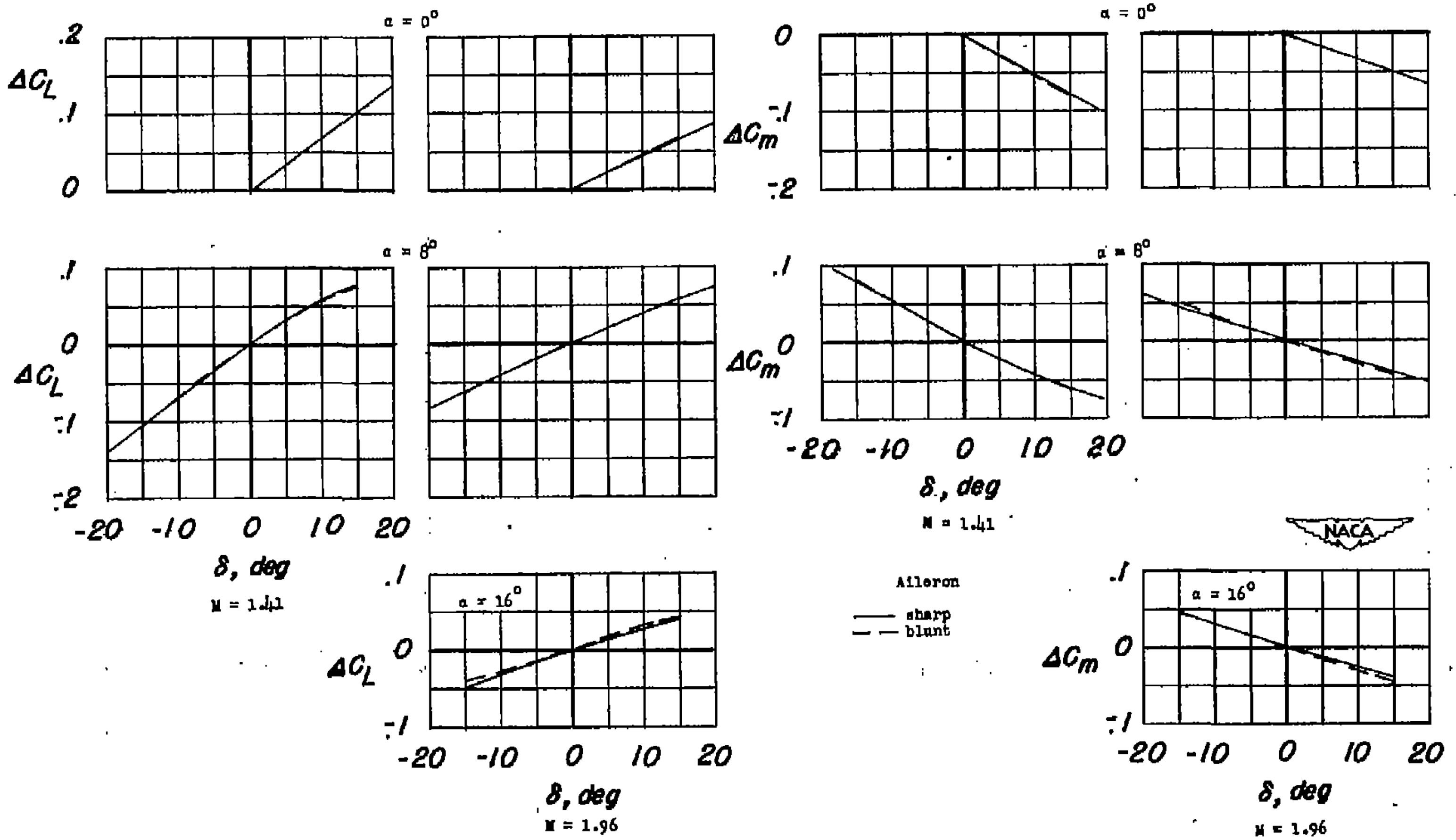

(b) ΔC_L and ΔC_m plotted against δ.

Figure 6.- Concluded.

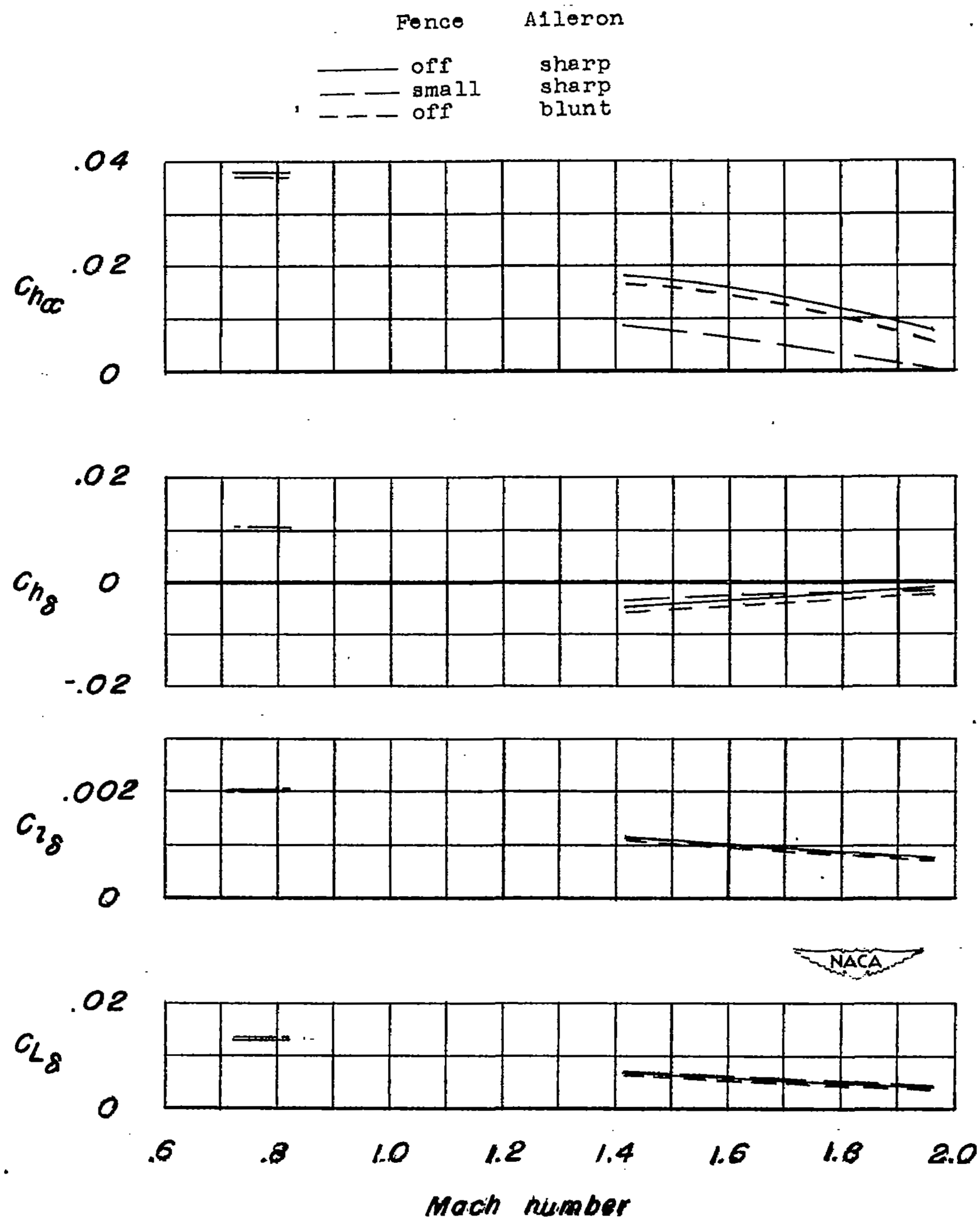

Figure 7.- Effects of a fence and of control trailing-edge bluntness on the variation with Mach number of the control hinge-moment and effectiveness parameters C_{h_α}, C_{h_δ}, C_{l_δ}, and C_{L_δ}. $\alpha = 0^\circ$; $\delta = 0^\circ$.

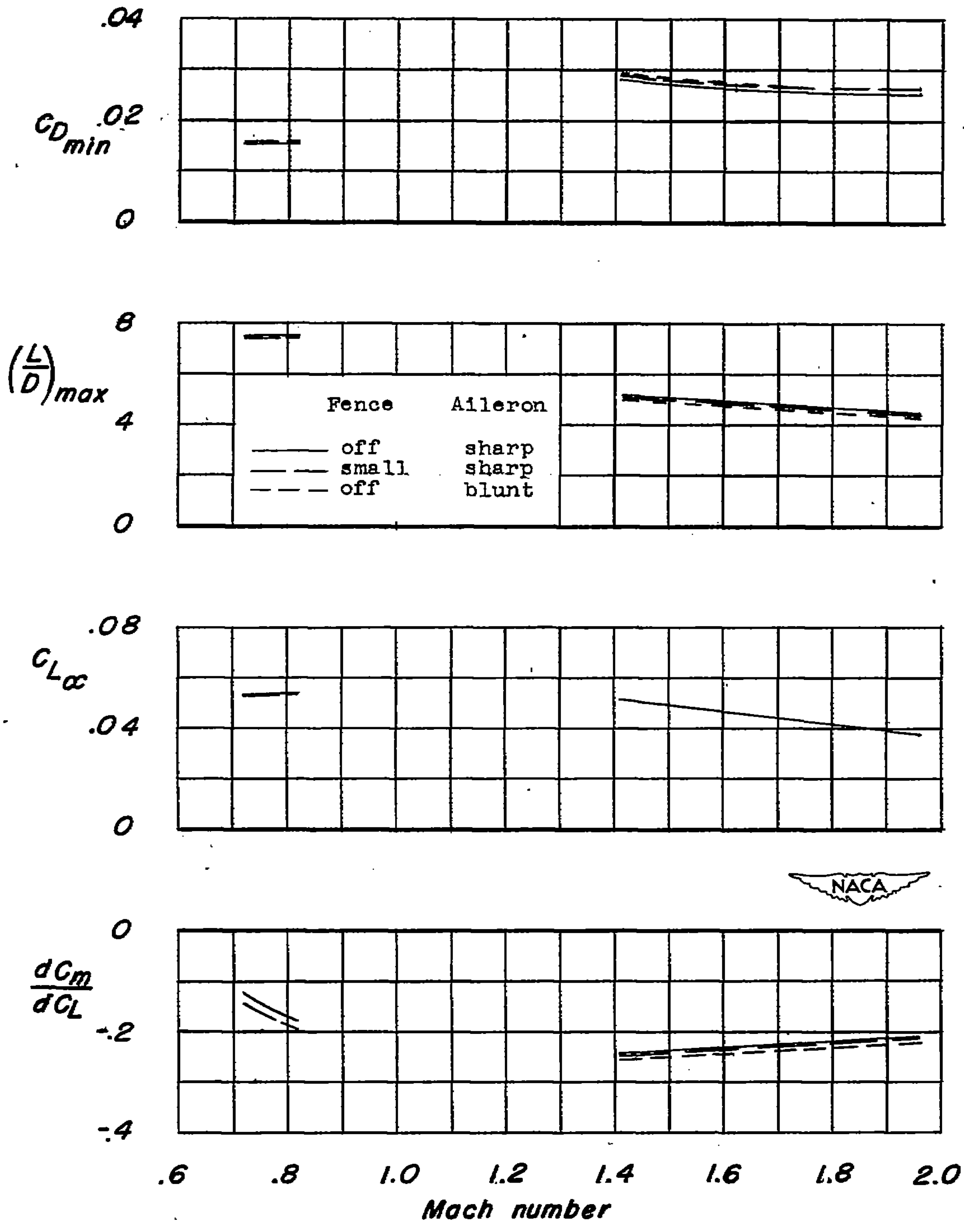

Figure 8.- Effects of a fence and of control trailing-edge bluntness on the variation with Mach number of the lift, drag, and pitching-moment characteristics of the wing-body combination. $\delta = 0^{\circ}$.

SECURITY INFORMATION

[redacted]

[redacted]